AGU PUBLICATIONS

JGR

Journal of Geophysical Research: Atmospheres

RESEARCH ARTICLE
10.1002/2013JD020822

Special Section:
The SPARC Data Initiative – Intercomparison of Vertically Resolved Chemical Trace Gas and Aerosol Climatologies

Key Points:
- First comprehensive intercomparison of UTLS ozone climatologies
- Compares climatologies from limb sounders to the TES nadir sounder
- Accounts for differences in vertical resolution

Correspondence to:
J. L. Neu,
jessica.l.neu@jpl.nasa.gov

Citation:
Neu, J. L., et al. (2014), The SPARC Data Initiative: Comparison of upper troposphere/lower stratosphere ozone climatologies from limb-viewing instruments and the nadir-viewing Tropospheric Emission Spectrometer, *J. Geophys. Res. Atmos.*, *119*, 6971–6990, doi:10.1002/2013JD020822.

Received 4 SEP 2013
Accepted 28 APR 2014
Accepted article online 4 MAY 2014
Published online 12 JUN 2014

The SPARC Data Initiative: Comparison of upper troposphere/lower stratosphere ozone climatologies from limb-viewing instruments and the nadir-viewing Tropospheric Emission Spectrometer

J. L. Neu[1], M. I. Hegglin[2], S. Tegtmeier[3], A. Bourassa[4], D. Degenstein[4], L. Froidevaux[1], R. Fuller[1], B. Funke[5], J. Gille[6], A. Jones[7], A. Rozanov[8], M. Toohey[3], T. von Clarmann[9], K. A. Walker[7], and J. R. Worden[1]

[1]Jet Propulsion Laboratory, California Institute of Technology, Pasadena, California, USA, [2]Department of Meteorology, University of Reading, Reading, UK, [3]GEOMAR Helmholtz Centre for Ocean Research, Kiel, Germany, [4]Department of Physics and Engineering Physics, University of Saskatchewan, Saskatoon, Saskatchewan, Canada, [5]Instituto de Astrofisica de Andalucia, CSIC, Granada, Spain, [6]Department of Oceanic and Atmospheric Sciences, University of Colorado Boulder, Boulder, Colorado, USA, [7]Department of Physics, University of Toronto, Toronto, Ontario, Canada, [8]Department of Physics and Electrical Engineering, University of Bremen, Bremen, Germany, [9]Department of Physics, Karlsruhe Institute of Technology, Karlsruhe, Germany

Abstract We present the first comprehensive intercomparison of currently available satellite ozone climatologies in the upper troposphere/lower stratosphere (UTLS) (300–70 hPa) as part of the Stratosphere-troposphere Processes and their Role in Climate (SPARC) Data Initiative. The Tropospheric Emission Spectrometer (TES) instrument is the only nadir-viewing instrument in this initiative, as well as the only instrument with a focus on tropospheric composition. We apply the TES observational operator to ozone climatologies from the more highly vertically resolved limb-viewing instruments. This minimizes the impact of differences in vertical resolution among the instruments and allows identification of systematic differences in the large-scale structure and variability of UTLS ozone. We find that the climatologies from most of the limb-viewing instruments show positive differences (ranging from 5 to 75%) with respect to TES in the tropical UTLS, and comparison to a "zonal mean" ozonesonde climatology indicates that these differences likely represent a positive bias for $p \leq 100$ hPa. In the extratropics, there is good agreement among the climatologies regarding the timing and magnitude of the ozone seasonal cycle (differences in the peak-to-peak amplitude of $<15\%$) when the TES observational operator is applied, as well as very consistent midlatitude interannual variability. The discrepancies in ozone temporal variability are larger in the tropics, with differences between the data sets of up to 55% in the seasonal cycle amplitude. However, the differences among the climatologies are everywhere much smaller than the range produced by current chemistry-climate models, indicating that the multiple-instrument ensemble is useful for quantitatively evaluating these models.

1. Introduction

Ozone is the third largest component of radiative forcing [*Solomon et al.*, 2007], with maximum radiative effect in the upper troposphere and lower stratosphere (UTLS) [*Forster and Shine*, 2002]. Yet the processes that control the UTLS distribution of ozone and its trends and variability, including the exchange of air between the stratosphere and troposphere, are not well quantified [*World Meteorological Organization*, 2011]. The UTLS region is characterized by strong vertical and horizontal ozone gradients and complex and rapidly evolving small-scale features such as tropopause folds [*Gettelman et al.*, 2011, and references therein]. Aircraft measurements are well suited for characterizing UTLS chemistry and dynamics because of their high spatial and temporal resolution. However, aircraft have only sparsely sampled the UTLS, raising questions about the representativeness of these measurements for applications such as evaluating free-running global chemistry-climate models [*Stratosphere-troposphere Processes and their Role in Climate Chemistry-Climate Model Validation (SPARC CCMVal)*, 2010; *Hegglin et al.*, 2010]. Current satellite instruments lack the spatiotemporal resolution to resolve some UTLS features, such as thin, highly dynamic filaments. Furthermore, they can have low signal-to-noise in the UTLS because of the small ozone abundance there relative to the middle stratosphere, and clouds can interfere with trace gas retrievals. However, satellites provide much greater spatial and temporal

coverage than aircraft, at a vertical resolution that is commensurate with that of most models [*SPARC CCMVal*, 2010; *Hegglin et al.*, 2010], and their measurements have provided extensive improvements in our understanding of UTLS structure and processes [e.g., *Hegglin et al.,* 2009; *Manney et al.,* 2011; *Peevey et al.*, 2012].

The purpose of the SPARC Data Initiative (M. I. Hegglin and S. Tegtmeier, SPARC Data Initiative report on the evaluation of trace gas and aerosol climatologies from satellite limb sounders, manuscript in preparation, 2014; M. I. Hegglin et al., SPARC Data Initiative: A multi-instrument comparison of stratospheric limb measurements, manuscript in preparation, *Journal of Geophysical Research*, 2014) is to better understand the differences between measurements of stratospheric trace gases and aerosols from different satellite instruments in order to reduce uncertainties in model evaluations, trends, and process studies. *Tegtmeier et al.* [2013] provides a detailed description and comparison of the ozone climatologies from limb-viewing instruments submitted to the Data Initiative, with a primary focus on the stratosphere. Here we compare the climatologies from six limb-viewing instruments (Atmospheric Chemistry Experiment-Fourier Transform Spectrometer (ACE-FTS), Aura-Microwave Limb Sounder (MLS), High Resolution Dynamics Limb Sounder (HIRDLS), Michelson Interferometer for Passive Atmospheric Sounding (MIPAS), Optical Spectrograph and Infrared Imager System (OSIRIS), and Scanning Imaging Absorption Spectrometer for Atmospheric Chartography (SCIAMACHY)), with vertical ranges that extend into the UTLS, to those from the nadir-viewing Tropospheric Emission Spectrometer (TES) instrument over 300–70 hPa for 2005–2010. The TES instrument is focused on tropospheric composition. Its ozone measurements have good sensitivity from the surface to 10 hPa and are well validated against ozonesondes in the UTLS [*Nassar et al.*, 2008; *Boxe et al.*, 2010], as discussed in section 2.1. Because TES is nadir viewing, it has relatively coarse vertical resolution (~6–7 km) compared to the limb-viewing instruments discussed here, most of which have vertical resolution of ~2–4 km. While TES has much finer horizontal resolution ($<$10 km) than the limb sounders (~200 km), the spacing between measurements is 182 km; thus, its ability to resolve horizontal features is not much different than that of the limb sounders.

Assessing the differences between satellite measurements in the UTLS is critical to advancing our understanding of this region and evaluating UTLS processes in models because uncharacterized biases in satellite data can lead to incorrect conclusions about UTLS chemistry or radiative forcing. However, given the strong gradients and small-scale structure of trace gas fields in the UTLS, differences in sampling and in vertical and horizontal resolution among instruments can lead to large differences that reflect sampling or smoothing error rather than systematic bias. *Toohey et al.* [2013] addresses the issue of sampling bias and shows, for example, that the construction of the zonal mean climatologies used here leads to biases of a few percent in the subtropical jet regions (~30°N and S) due to a combination of the sloping ozone surfaces in these regions and the increase in sampling density with latitude. To address differences in vertical resolution, one approach is to smooth the measurements to a common resolution, which allows for an "apples-to-apples" comparison [*Rodgers and Connor*, 2003]. Here we use the TES observational operator (averaging kernel + constraint) to vertically smooth the climatologies from the limb sounders and provide a common basis for assessment of systematic differences in large-scale vertical and horizontal gradients as well as seasonal and interannual variability of ozone within the UTLS.

We use TES data as the common reference because TES ozone data have been extensively validated against ozonesondes for a wide range of geophysical states and latitudes. Studies have shown that there are no observable changes in biases in the TES ozone data over time, and the bias is well characterized as a function of latitude [*Worden et al.*, 2007; *Verstraeten et al.*, 2013]. In addition, the sonde comparisons indicate that the calculated random errors are in agreement with actual errors. This means that evaluating other satellite measurements against TES provides an assessment of instrument bias rather than unquantified errors in the TES retrieval.

TES measures over the entire wavelength range of ozone infrared absorption and can thus provide the sensitivity of outgoing longwave radiation (OLR) to the vertical distribution of ozone [*Worden et al.*, 2008, 2011]. As part of the Atmospheric Chemistry and Climate Model Intercomparison Project (ACCMIP) TES tropospheric ozone and its effect on OLR have been compared to the same quantities derived from models and used to reduce uncertainties in ozone radiative forcing [*Bowman et al.*, 2013]. TES is also extensively used for the evaluation of upper tropospheric ozone and its precursors in chemistry transport models [e.g., *Jones et al.*, 2009]. Assessing the differences between TES and other instruments measuring ozone in the UTLS region will provide a better understanding of the ozone gradients and variability that TES fails to capture due

Table 1. Information on Limb-Viewing Instruments[a]

Instrument and Data Version	Vertical Range	Vertical Resolution	References
ACE-FTS v2.2 update	5–95 km	3–4 km	*Dupuy et al.* [2009]
Aura-MLS v2.2	12–75 km	3 km	*Froidevaux et al.* [2008] and *Jiang et al.* [2007]
HIRDLS v6.0	10–55 km	1 km	*Nardi et al.* [2008] and *Gille et al.* [2008]
MIPAS v220	6–70 km	2.7–3.5 km	*von Clarmann et al.* [2009]
OSIRIS v5-0	10–60 km	2 km	*Degenstein et al.* [2009]
SCIAMACHY v2.5	10–60 km	3–5 km	*Mieruch et al.* [2012]

[a]Data version, vertical range, vertical resolution, and references for the six limb-viewing instruments used in this study.

to its coarse resolution. Furthermore, improved characterization of satellite measurements of ozone in this region will allow us to better quantify the significance of model-measurement differences in precursor emissions and radiative forcing in the UTLS.

2. Data

Detailed information on the limb-viewing satellite instruments used here (ACE-FTS, Aura-MLS, HIRDLS, MIPAS, OSIRIS, and SCIAMACHY) can be found in M. I. Hegglin et al. (manuscript in preparation, 2014), while *Tegtmeier et al.* [2013] provide a discussion of their ozone measurements and SPARC Data Initiative ozone climatologies. The data versions used here are the same as those in *Tegtmeier et al.* [2013] (Table 1). The climatologies consist of zonal monthly mean ozone abundances for 36 latitude bins (midpoints at 87.5°S, 82.5°S, …, 87.5°N) calculated on a standard pressure grid, with 11 levels where $p \geq 70$ hPa (300, 250, 200, 170, 150, 130, 115, 100, 90, 80, and 70 hPa). *Toohey et al.* [2013] and *Funke and von Clarmann* [2012] discuss potential errors in constructed climatologies due to differences in instrument sampling and averaging technique, respectively.

2.1. TES Ozone Measurements

TES is a Fourier transform spectrometer that was launched on the NASA Earth Observing System Aura satellite in 2004 [*Beer*, 2006; *Beer et al.*, 2001]. The Aura satellite is in a Sun-synchronous polar orbit with equator crossing times of ~13:43 (ascending node) and ~1:43 (descending node) and a 16 day repeat cycle. TES measures in the thermal infrared (650–3050 cm^{-1}) with a spectral resolution of 0.06 cm^{-1} and provides line-width-limited discrimination of radiatively active species, including O_3, CO, H_2O, HDO, CH_4, CO_2, NH_3, CH_3OH, and HCOOH, with greatest sensitivity in the troposphere. At the nadir, the horizontal resolution is 0.5 × 5 km, and the footprint is 5.3 × 8.5 km, with a separation of ~182 km between consecutive measurements. In cloud-free conditions, TES nadir ozone profiles have approximately 4 degrees of freedom for signal, with ~2 in the troposphere and ~2 in the stratosphere (below ~5 hPa), equivalent to a vertical resolution of ~6–7 km (Figure 1a). While TES measures in both Global Survey and Special Observations modes, here we use only global survey data, which provide near-global coverage in 16 orbits (~26 h). The retrievals and error estimation are based on the optimal estimation approach [*Rodgers*, 2000] and are described in *Worden et al.* [2004], *Bowman et al.* [2002, 2006], and *Kulawik et al.* [2006]. TES data, including averaging kernels and error covariance matrices, are publicly available. For more information, see http://tes.jpl.nasa.gov/.

We use TES data covering the period July 2005 to December 2010. TES provides global coverage from July 2005 through May 2008. To extend the life of the instrument, the latitudinal coverage was reduced in June 2008 to 60°S–82°N and in July 2008 to 50°S–70°N. From January to April 2010, the instrument went offline due to problems with the scanning mechanism. When operations resumed in May 2010, the latitude coverage was further reduced to 30°S–50°N and the calibration strategy was changed to reduce wear on the pointing mechanism of the instrument. Reducing the number of calibration scans resulted in a 25% increase in the number of observations per global survey and regular but nonuniform spacing between the measurements (ground track separation cycles through 56 km, 195 km, 187 km, and 122 km and then returns to 56 km), with no discernible impact on data quality [e.g., *Verstraeten et al.*, 2013]. A second data gap of ~3 weeks occurred in October 2010, with only two Global Surveys conducted that month.

The TES SPARC Data Initiative ozone climatology is based on Level 2 version 4 (V4) data [*Boxe et al.*, 2010]. Vertical profiles are retrieved as log(vmr), where vmr is volume mixing ratio, on a 67 Level pressure grid, and are interpolated in log(pressure) to the SPARC Data Initiative pressure grid. Only retrievals that pass the master quality flag have been used, and there is an additional screening to eliminate "C curve" ozone profiles.

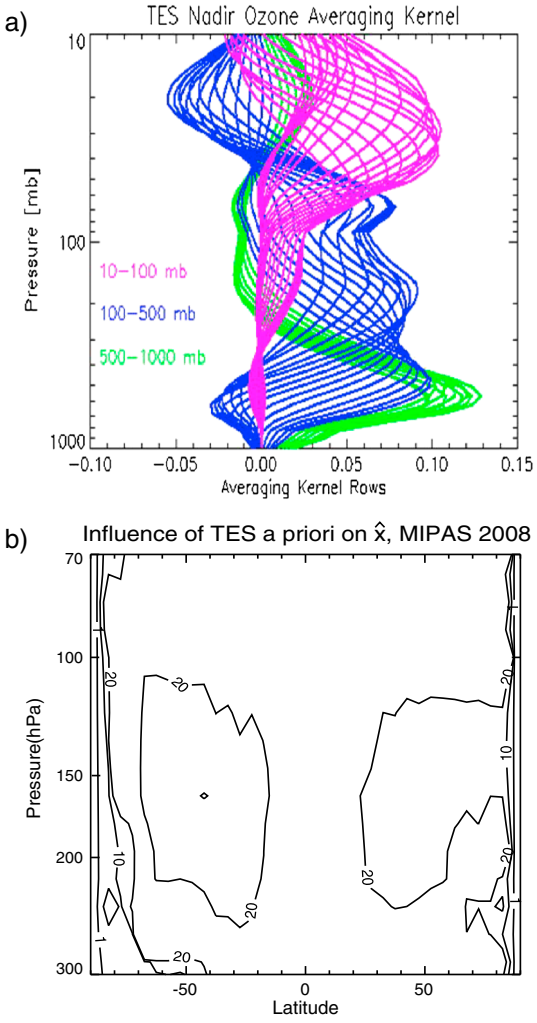

Figure 1. (a) Sample TES averaging kernel. The lines show the relative contribution of the true mixing ratio at each pressure level to the retrieved mixing ratio at 500–1000 hPa (green), 100–500 hPa (blue), and 10–100 hPa (purple). TES ozone averaging kernels vary with temperature, surface properties, clouds, and ozone. (b) Influence of the TES a priori on the virtual retrieval for MIPAS. Annual mean value of the ratio of *Ax*, the contribution of the original climatology to the virtual retrieval, to $x^a - Ax^a$, the contribution of the TES a priori to the virtual retrieval, for MIPAS for 2008. Results are very similar for other instruments and years. When the ratio is close to 1, the terms are of similar magnitude so that the a priori and true profiles contribute equally to the retrieved ozone. Contour values of 1, 10, and 20 are shown.

These profiles, which represent approximately 1–2% of TES V4 ozone data, result from nonlinearities in the retrieval in the presence of clouds. These nonlinearities can lead to convergence to an unphysical state in which the ozone profile takes on a "C" shape under particular thermal conditions. While we do not perform any cloud screening in the selection of profiles for the climatology, the master quality flag does screen out profiles with cloud optical depth >50 from 975 to 1200 cm^{-1}.

TES measurements are retrieved, and thus typically averaged in, log-space. However, for proper comparison to other data sets shown here, we have used linear averaging. Simple unweighted means of the available data are calculated for each month and latitude bin. A minimum of five observations per bin is required, but in practice the minimum number of profiles is 28, and in most cases the number is >1000.

TES ozone measurements have been extensively validated against ozonesondes [*Nassar et al.*, 2008; *Boxe et al.*, 2010; *Verstraeten et al.*, 2013]. In the 300–70 hPa region evaluated here, TES is positively biased with respect to sondes in all latitude regions except the southern low and middle latitudes (15–60°S), where it is negatively biased. The mean bias is smaller than 20% in all latitude regions. In the northern midlatitudes, the bias is +15–20% for 100 hPa $< p <$ 300 hPa and $<$ +5% for 70 hPa $< p <$ 100 hPa. The bias curve is "c shaped" in the southern midlatitude UTLS, with near-zero bias at 300 and 70 hPa and a maximum value of −20% at 150 hPa. In the tropical UTLS, TES shows a small positive bias ($<$10%) with respect to sondes. An analysis of seasonal variations in the northern midlatitude (35–56°N) bias showed relatively small seasonal differences, except during summer when the bias decreases to $<$10% everywhere. In this paper, we include a comparison of the SPARC Data Initiative climatologies to a "zonal mean" ozonesonde climatology (sections 3.4 and 3.5) and find different biases for the TES climatology than those reported in the TES validation literature in some regions. These differences likely result from not accounting for (1) the sampling locations of the ozonesonde profiles and (2) the difference in vertical resolution between TES and the sondes in the climatological comparisons.

2.2. Use of Zonal Mean Monthly Mean Averaging Kernels

As discussed above, TES retrievals use the optimal estimation technique, with the retrieved profile, $\hat{x}$ (ln(vmr)), given by the following:

$$\hat{x} = x^a + A^{xx}(x - x^a)$$

where x (ln(vmr)) is the true state, x^a (ln(vmr)) is the a priori profile, and A^{xx} is the averaging kernel matrix. For the comparisons shown here, the climatologies of the higher vertical resolution limb-viewing instruments are

taken to be the "true" state, x, and the TES observational operator (a priori and averaging kernel) are used to simulate a "virtual" TES retrieval, $\hat{x}$. Normally, this type of comparison is done on a profile-by-profile basis. However, due to the large number of instruments involved in this comparison and the focus on zonal mean climatologies, we apply the monthly mean zonal mean observational operator to the monthly mean zonal mean SPARC Data Initiative climatologies. The use of monthly mean zonal mean averaging kernels can be justified by the fact that the variations in TES averaging kernels are not highly correlated with variations in ozone. In the troposphere, ozone explains less than 25% of the variance in the averaging kernel diagonal at all latitudes due to the strong dependence of the averaging kernels on clouds, water vapor, and temperature, as discussed by *Aghedo et al.* [2011]. In the UTLS region, ozone explains up to 35% of the variance in the averaging kernel diagonal in midlatitudes, with a minimum value at ~150–200 hPa where the sensitivity is relatively low and the a priori has a significant impact on the retrievals (see below). In the tropical UTLS, ozone explains 20–60% of the variance in the averaging kernel diagonal, with maximum correlation at ~150 hPa. However, at all latitudes the dependence of the averaging kernel diagonal on ozone abundance is weak for ozone within 40% of the mean value at each level; the correlations are primarily driven by ozone abundances more than 40% higher than the mean value. In the midlatitudes, ozone abundances that are twice as large as the mean value at a given pressure level have a ~30% higher averaging kernel diagonal value. In the tropics the slope of the relationship is somewhat higher, and a 100% increase in ozone over the mean value is associated with a 45% larger averaging kernel diagonal.

Aghedo et al. [2011] examined the error associated with using monthly mean averaging kernels in two climate models for $p \geq 100$ hPa. They found differences in ozone of at most 3% when using monthly mean as compared to time-varying averaging kernels. To test the error involved in using zonal mean averaging kernels with zonal mean data, we examined the difference between TES and Aura-MLS measurements for 2006 gridded at $5° \times 10°$, using the $5° \times 10°$ gridded TES averaging kernels to smooth the Aura-MLS measurements. The zonal mean of this difference is always within 10% of the difference between zonal mean TES and Aura-MLS measurements using zonal mean averaging kernels, and furthermore, the difference in the zonal mean data sets is always less than the difference in gridded data sets except in high southern latitudes during October. In addition, the difference between using zonal mean averaging kernels aggregated from individual profiles and using the zonal mean of the gridded averaging kernels is negligible (<2% everywhere). We therefore conclude that using zonal mean averaging kernels with zonal mean data provides a lower estimate that is within ~10% of the true difference between each instrument and TES. However, we note that because the averaging kernels are not fully independent of the ozone abundance, comparison using the TES observational operator may not accurately reflect the difference between TES and another instrument if there are large systematic differences between them. Given the fact that the averaging kernels depend only weakly on the ozone abundance for ozone within 40% of the mean value, we do not expect this to be an issue except where instruments differ from TES by more than 40%. In such cases, which are rare (see the discussion of Figure 4 below), the error associated with using an averaging kernel that has sensitivity that is not appropriate for the ozone observed by the other instrument can only be quantified by recalculating the averaging kernel to "match" the instrument's ozone, which is beyond the scope of this paper.

2.3. Applying the TES Observational Operator

For each instrument, we interpolate the monthly mean zonal mean climatologies from the SPARC pressure grid to the TES retrieval levels (67 levels between the surface and 0.1 hPa). We fill in the levels below the lowest measurement in each latitude bin using the monthly mean, zonal mean TES a priori as a "fill profile." The virtual TES retrievals are calculated and then interpolated back to the SPARC pressure grid, and we average over all of the available data from 2005 to 2010 to create the climatologies shown here. We use the a priori as a fill profile because it makes $A(x - x^a) = 0$ in the troposphere (defined as $p \geq p_{max}$ for each instrument) since $x = x^a$ there, which is equivalent to applying the observational operator only to the levels where the limb-viewing instruments provide measurements. However, the fill profile can still impact the comparison to TES due to the vertical smearing of the averaging kernels. The difference between the virtual retrieval for a given instrument ($\hat{x}_{INST}$) and TES ($\hat{x}_{TES}$) can be written as

$$\hat{x}_{INST} - \hat{x}_{TES} = A^{SS}\left(x_{True}^{STRAT} - x_{INST}^{STRAT}\right) - A^{ST}\left(x_{True}^{TROP} - x_{INST}^{TROP}\right)$$

where A^{SS} is the "stratospheric" component of the averaging kernel matrix ($p < p_{max}$), x_{INST}^{STRAT} is the ozone profile measured by the limb-viewing instrument, A^{ST} represents the cross terms of the averaging kernel that define the tropospheric influence on the stratosphere, and x_{INST}^{TROP} is the fill profile. To test the sensitivity of our results to our approach of using the TES a priori to fill in the profiles below the lowest measurement level, we have also calculated virtual retrievals in which we scale the TES a priori using the percent difference between the ozone value at p_{max} for each latitude bin for each of the other instruments and the TES a priori at this same latitude and pressure. Comparison of the virtual retrievals using the two different filling methods allows us to identify regions where our results are highly dependent on our assumptions for $p > p_{max,}$ as discussed below.

3. Intercomparison of Zonal Mean Ozone Climatologies

As in *Tegtmeier et al.* [2013], we use a series of diagnostics to evaluate differences in the vertical, latitudinal, and temporal structure of ozone as represented by the SPARC Data Initiative climatologies. These diagnostics include zonal mean cross sections, vertical and latitudinal profiles, seasonal cycles, and interannual variability. However, rather than examining differences from the multi-instrument mean, we use the TES climatology as the standard to which the other climatologies are compared and, in some cases, include climatological ozonesonde measurements as an additional validation tool. We also analyze the impact of the TES observational operator on the climatologies from the limb-viewing instruments and assess how the use of the observational operator affects the ozone intercomparison.

3.1. Zonal Mean Cross Sections

Figure 2 (left) shows the zonal mean ozone climatology for each instrument from 300 to 70 hPa averaged over 2005–2010 (2005–2007 for HIRDLS) using the data directly from the SPARC Data Initiative archive. All of the instruments show similar features, including the typical low tropical values, strong subtropical gradients, and relatively flat midlatitude isopleths that reflect the competing effects of the stratospheric overturning circulation and mixing with the troposphere. The instruments also all show lower ozone values in the Southern Hemisphere than in the Northern Hemisphere in the annual mean due to the asymmetry in the overturning circulation. A few instruments show features not seen in the climatologies from any of the other instruments. The MIPAS climatology has an unusual contour shape in the tropics between ~200 and 100 hPa, with a slight "double ear" structure in the subtropics and a deep minimum near the equator, and Aura-MLS has very flat, tightly spaced contours near 100 hPa. It is likely that some of the differences in the climatologies in the upper tropical troposphere arise from differences in the impact of clouds on the retrievals and in criteria used for cloud screening, which can cause sampling artifacts (T. von Clarmann, personal communication, 2013). The OSIRIS climatology has an unusually strong zonal gradient at ~75°N below 250 hPa, which appears to reflect sampling bias in the climatology resulting from a lack of measurements in polar winter [*Toohey et al.,* 2013].

3.2. Impact of TES Observational Operator

Figure 2 (middle) shows the virtual retrievals using the TES observational operator, and Figure 2 (right) shows the percent difference between the virtual TES retrieval (VTR) and the original climatology (OC) for each instrument ($100 \times (VTR - OC)/OC$). Hatched regions in Figure 2 (right) indicate where the choice of fill profile (TES a priori or scaled a priori) has a significant impact on the VTR, quantified (arbitrarily) as where the difference between the VTRs using the two fill profiles exceeds 10%. The HIRDLS climatology shows the most uniform and smallest changes in ozone after the application of the TES observational operator. The operator acts to smooth out the small-scale features seen in the MIPAS, Aura-MLS, and OSIRIS climatologies, as seen in Figure 2 (middle), due to the vertical smearing of the broad averaging kernels. In the tropics, the observational operator tends to increase ozone for $p \leq 80$ hPa and decrease it for $p > 80$ hPa relative to the original climatologies (with strong increases at 100 hPa associated with the unusual features in MIPAS and Aura-MLS). MIPAS and Aura-MLS are the only two instruments for which the choice of the fill profile has a significant impact in the tropics. It is unclear why this is the case for Aura-MLS, but the MIPAS tropical ozone values are very low at $p > 250$ hPa compared to the other instruments, and there is a very large difference between the TES a priori and the a priori scaled using the MIPAS measurements in this region.

In the extratropics, the observational operator tends to increase ozone at ~150 hPa and decrease it above and below, which increases the vertical and horizontal gradients of ozone in the virtual retrievals compared to the

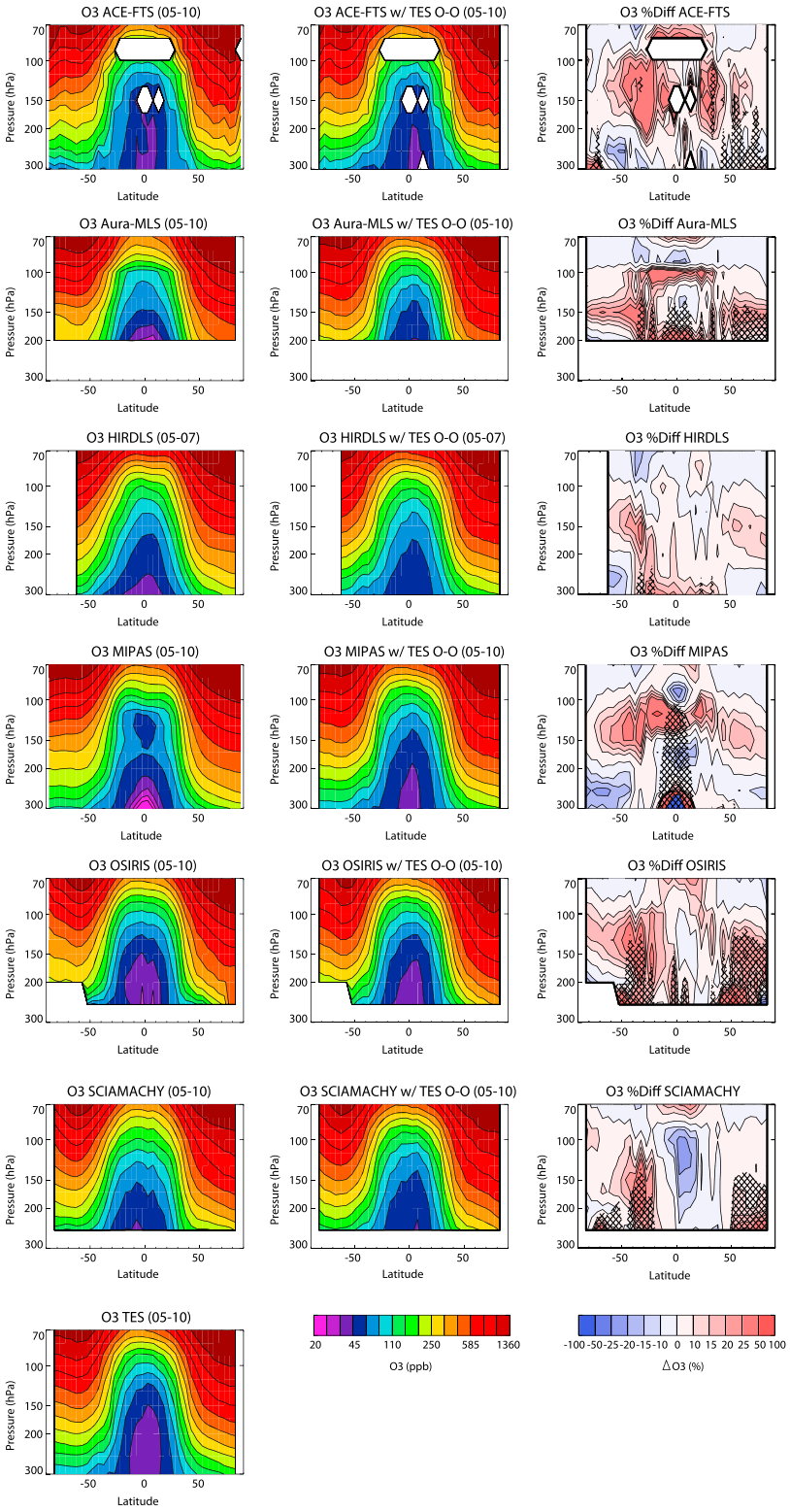

Figure 2. Cross sections of annual mean zonal mean ozone from 300 to 70 hPa for 2005–2010. (left) Ozone cross sections from ACE-FTS, Aura-MLS, HIRDLS (2005–2007), MIPAS, OSIRIS, SCIAMACHY, and TES. (middle) Cross sections from ACE-FTS, Aura-MLS, HIRDLS, MIPAS, OSIRIS, and SCIAMACHY after application of the TES observational operator. (right) Percent change in annual mean zonal mean ozone introduced by the TES observational operator ($100 \times (\mathrm{VTR} - \mathrm{OC})/\mathrm{OC}$, where VTR = virtual TES retrieval and OC = original climatology). Hatching indicates regions where the difference between the virtual retrievals using the TES a priori as the fill profile and those using the scaled a priori as the fill profile exceeds 10%. See text for details.

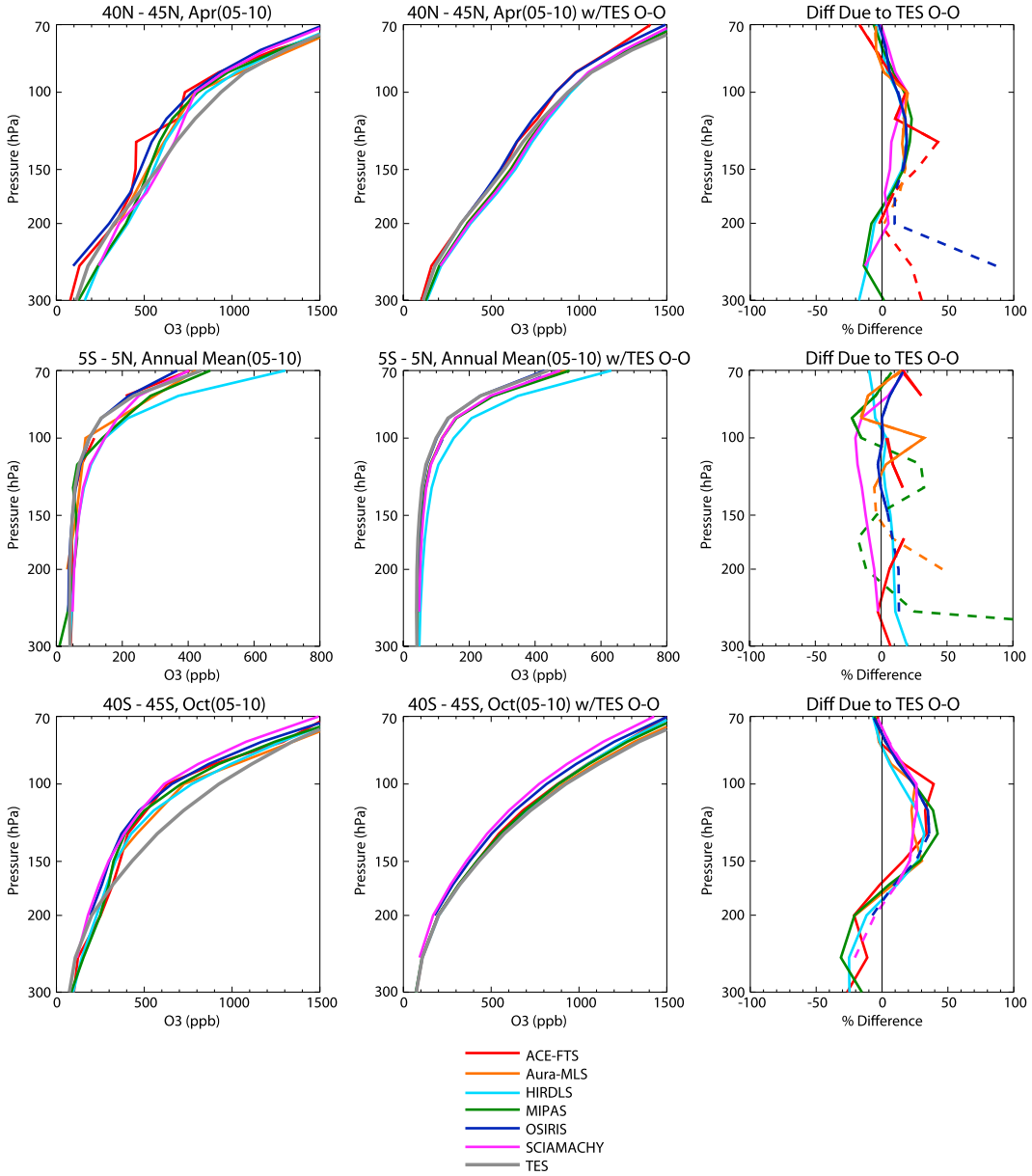

Figure 3. Vertical profiles of zonal mean ozone for 2005–2010. (left column) Ozone profiles from the original climatology for each instrument. (middle column) Ozone profiles after application of the TES observational operator. TES measurements are the same as in the Figure 3 (left column). (right column) The percent change in the ozone profiles introduced by the TES observational operator for all instruments except TES ($100 \times (\mathrm{VTR} - \mathrm{OC})/\mathrm{OC}$). Dashed lines indicate portions of the profile where the difference between the virtual retrievals using the TES a priori as the fill profile and those using the scaled a priori as the fill profile exceeds 10%. (top row) Zonal mean ozone profiles and differences for 40–45°N for April 2005–2010. (middle row) Annual mean zonal mean ozone profiles and differences for 5°S–5°N for 2005–2010. (bottom row) Zonal mean ozone profiles and differences for 40–45°S for October 2005–2010.

original climatologies. This increase in gradient clearly cannot result from the TES averaging kernels, which smooth and flatten vertical gradients. Rather, the increase results from the influence of the a priori; comparison of the terms Ax, the contribution of the true profile from each climatology to the virtual retrieval, and $x^a - Ax^a$, the contribution of the TES a priori to the virtual retrieval, (Figure 1b) shows that TES's sensitivity is lowest, and the a priori profile makes the largest contribution to $\hat{x}$, in the midlatitudes at ~150–200 hPa, as well as in the southern high latitudes at $p > 150$ hPa.

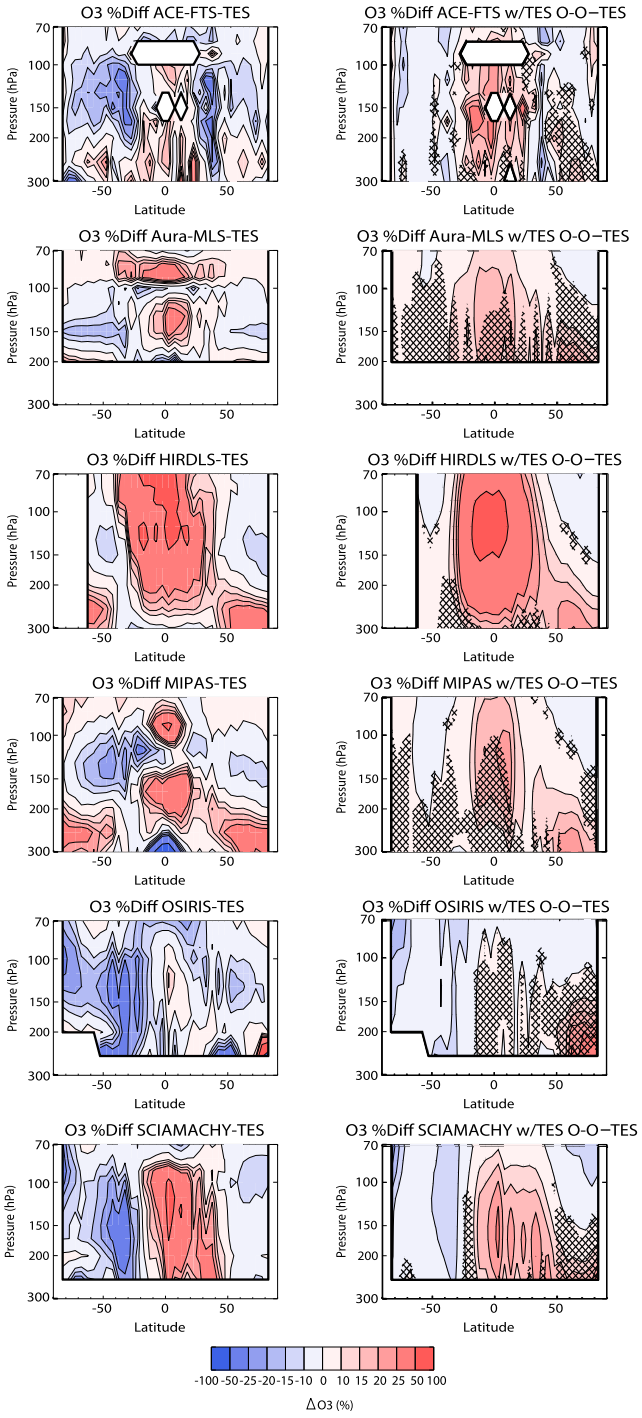

Figure 4. Cross sections of annual mean zonal mean ozone differences from 300 to 70 hPa for 2005–2010. (left) Annual mean zonal mean ozone percent differences between the climatology from each instrument and TES for 2005–2010 (HIRDLS: 2005–2007) (100 × (OC − TES)/TES). (right) Percent differences between the virtual retrieval from each instrument and TES after application of the TES observational operator (100 × (VTR − TES)/TES). Hatched regions indicate where the difference in the virtual retrieval using the two different fill profiles exceeds 50% of the difference between the virtual retrieval and TES.

The sensitivity to the fill profile is largest in the extratropics, in particular for the climatologies whose range does not extend to 300 hPa (Aura-MLS, OSIRIS, and SCIAMACHY). Between ~200 and 300 hPa there are large vertical gradients in midlatitude ozone that are not well represented by the TES a priori so that there is a large difference between the two fill profiles (the a priori and the scaled a priori). Furthermore, the averaging kernels spread the information from 300 hPa upward to ~100 hPa in the extratropics so that changing ozone at 300 hPa has a significant influence over a large vertical range.

Figure 3 shows a comparison of zonal mean vertical profiles in the northern midlatitudes (April), tropics (annual mean), and southern midlatitudes (October). Figure 3 (left column) is once again the original SPARC Data Initiative climatology for each instrument, while Figure 3 (middle and right columns) show the virtual retrievals using the TES observation operator and the percent difference between the virtual retrievals and the original data (100 × (VTR − OC)/OC), respectively. Dashed lines in Figure 3 (right column) indicate where the choice of fill profile affects the VTR by more than 10%. In the midlatitudes, the observational operator smoothes the vertical profiles; it decreases ozone for $p > 150$ hPa and increases it for $p < 150$ hPa for all instruments for which the virtual retrievals do not depend strongly on the fill profile. In the tropics, as discussed above, the observational operator acts to slightly increase ozone at $p < 80$ hPa and slightly decrease it at $p > 80$ hPa, as well as to smooth small-scale vertical structures.

3.3. Percent Difference From TES

Figure 4 shows the percent difference between the annual mean climatology for each instrument and TES (100 × (OC − TES)/TES, left) and the percent difference between the virtual retrievals for each instrument and TES (100 × (VTR-TES)/TES, Figure 4, right).

The hatched regions in Figure 4 (right) indicate where differences in the VTR due to the choice of fill profile exceed 50% of the difference between the VTR and TES for each instrument. While 50% is an arbitrary choice, it highlights a combination of regions where the fill profile has a >10% impact on the virtual retrievals (see Figure 2 above) and regions where differences between the virtual retrievals and TES are small so that even <10% differences due to the fill profile are large relative to VTR-TES. The original climatologies from all instruments except ACE-FTS and OSIRIS show positive differences of more than 25% with respect to TES in the tropics. However, except for HIRDLS, which is affected by uncorrected emission from aerosols in the tropics (J. Gille, private communication, 2013), the biases are not uniform in pressure, and there are some regions with negative biases, including for $p < 70$ hPa (which can impact the region of interest when the TES observational operator is applied). The virtual retrievals represent the combined influence of the vertical smoothing of the TES averaging kernel and the a priori, whose influence is not negligible due to TES's imperfect sensitivity. Together these act to both vertically smooth the differences from TES and reduce them to ≤ 25% for the virtual retrievals from all instruments except HIRDLS. However, for the Aura-MLS and MIPAS virtual retrievals, the biases with respect to TES are robust (i.e., not strongly dependent on the fill profile) only for $p <$ ~100 hPa. For ACE-FTS, which is a solar occultation instrument and has very sparse sampling in the tropics due to its orbit, the difference from TES may largely reflect a >5% tropical sampling bias in the climatology [*Toohey et al.,* 2013].

HIRDLS and MIPAS also have annual mean positive differences of 10–30% with respect to TES at $p \geq 150$ hPa in the northern middle and high latitudes. Again, the differences with respect to TES can be seen in the original climatologies, but the vertical extent of the positive biases is greater in the virtual retrievals. The climatologies from the other instruments also show positive differences from TES in the same region, but for the most part these are not seen in the original climatologies and are an artifact of the impact of the fill profile. In the Southern Hemisphere, the original climatologies are generally negatively biased with respect to TES, especially above 200 hPa. The TES observational operator strongly reduces the difference between the original data sets and TES in the Southern Hemisphere, such that the virtual retrievals agree with the TES climatology to within ~10%. This is likely because the differences between the original climatologies and TES occur largely in the region where TES has low sensitivity and the a priori plays an important role in the virtual retrievals (Figure 1b). OSIRIS and SCIAMACHY, which measure only in the sunlit portion of the atmosphere, have >5% negative sampling biases in their climatologies in the southern middle and high latitudes [*Toohey et al.,* 2013], which may at least partially explain their larger differences with respect to TES relative to the climatologies from other instruments.

3.4. Latitudinal Gradients on Pressure Surfaces

Figure 5 shows the 2005–2010 mean April ozone from each instrument as a function of latitude on four pressure surfaces. The original data sets (first column), virtual retrievals (second column), and percent differences between the original data sets and TES ($100 \times (\mathrm{OC} - \mathrm{TES})/\mathrm{TES}$, third column) and virtual retrievals and TES ($100 \times (\mathrm{VTR} - \mathrm{TES})/\mathrm{TES}$, fourth column) are all shown. Dashed lines in Figure 5 (fourth column) indicate where differences in the VTR due to the choice of fill profile exceed 50% of the difference between the VTR and TES for an instrument. In addition to the satellite climatologies, Figure 5 (first column) also includes a "zonal mean" ozone climatology from ozonesonde measurements at 48 stations from the data sets described by *Logan* [1999] (representative of 1980–1993) and *Thompson et al.* [2003] (representative of 1997–2011) (Table 2). We note that there are at most four ozonesonde stations in a given latitude band, and many latitude bands contain only one station, likely leading to large sampling biases. Furthermore, no attempt has been made to account for differences in vertical resolution between the satellites and the sondes, primarily because it is unclear whether the use of zonal mean averaging kernels would exacerbate the sampling bias. Nevertheless, we include the ozonesonde climatology to demonstrate the good agreement between the satellites and the sondes and to provide an additional tool to investigate biases in the satellite climatologies.

At $p \leq 200$ hPa, the absolute differences between the climatologies are mostly small, except at high latitudes ($>50^{o}$, Figure 5, first column). Given the large ozone abundance at high latitudes, however, the absolute differences between the instruments translate to small relative differences; the limb-viewing instruments agree with each other and with TES (Figure 5, third column) to within ~30% at middle and high latitudes for $p \leq 200$ hPa. The ozonesonde measurements suggest that the TES climatology is positively biased by ~20% in the Northern Hemisphere extratropics for 80 hPa $< p <$ 200 hPa, in good agreement with the TES validation

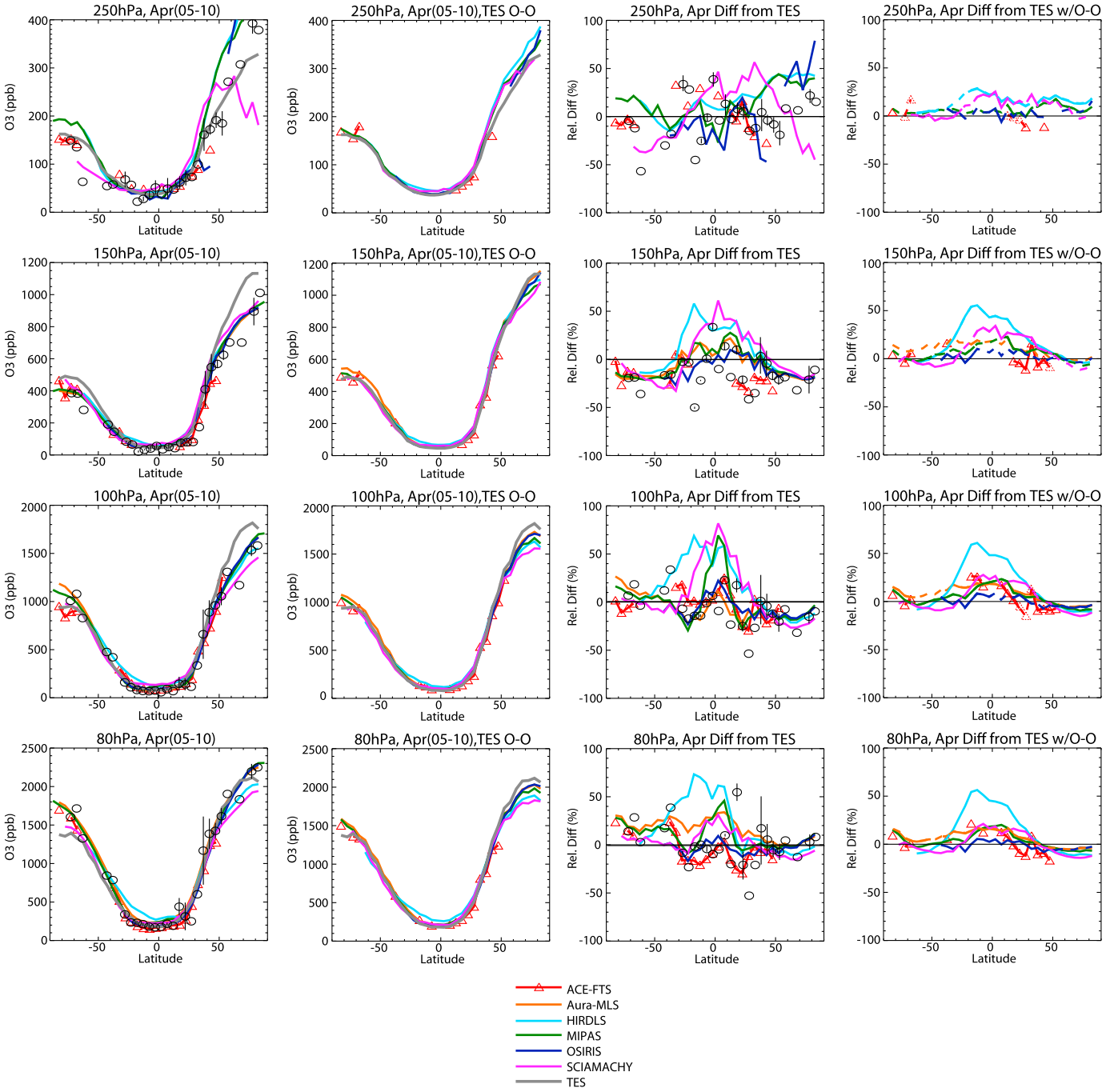

Figure 5. Meridional profiles of monthly mean zonal mean ozone for 2005–2010. (first column) Meridional zonal mean ozone profiles from the climatology for each instrument at (top row) 250 hPa, (second row) 150 hPa, (third row) 100 hPa, and (bottom row) 80 hPa for April 2005–2010. Black circles show the ozonesonde climatology; vertical bars represent the standard deviation of climatological mean values for latitude bands with more than one station. (second column) Meridional profiles after application of the TES observational operator to climatologies from each instrument. The TES measurements are the same as in Figure 5 (first column). (third column) Percent difference between each instrument and TES as a function of latitude on each pressure surface. (100 × (OC − TES)/TES) Black circles show the ozonesonde climatology; vertical bars are as above. (fourth column) Same as Figure 5 (third column) but for virtual retrievals with the TES observational operator applied (100 × (VTR − TES)/TES). Dashed lines indicate portions of the virtual retrieval where the difference in the virtual retrieval using the two different fill profiles exceeds 50% of the difference between the virtual retrieval and TES.

Table 2. Station Information for the Ozonesonde Climatology[a]

Station Name	Latitude	Longitude	Soundings/Month	Data Record	Latitude Bin
Forster[b]	71°S	12°E	28	1985–1991	70–75°S
Syowa[b]	69°S	39°E	18	1986–1993	65–70°S
Marambio[b]	64°S	57°W	20	1988–1995	60–65°S
Lauder[b]	*45°S*	*170°E*	*24*	*1986–1990*	*45–50°S*
Asp_Laverton[b]	*38°S*	*145°E*	*24*	*1980–1995*	*35–40°S*
Pretoria[b]	26°S	28°E	11	1990–1993	25–30°S
Irene[c]	26°S	28°E	19	1998–2012	25–30°S
La Reunion[c]	21°S	56°E	31	1998–2012	20–25°S
Suva[c]	18°S	178°E	22	1998–2011	15–20°S
Tahiti[c]	18°S	149°W	6	1998–1999	15–20°S
Am. Samoa (Thompson)[c]	*14°S*	*170°W*	*37*	*1998–2012*	*10–15°S*
Am. Samoa (Logan)[b]	*14°S*	*170°W*	*13*	*1986–1996*	*10–15°S*
Ascension Island[c]	*8°S*	*14°W*	*45*	*1998–2010*	*5–10°S*
Watukosek[c]	*8°S*	*113°E*	*24*	*1998–2012*	*5–10°S*
Natal (Logan)[b]	*6°S*	*35°W*	*23*	*1978–1992*	*5–10°S*
Natal (Thompson)[c]	*5°S*	*35°W*	*39*	*1998–2011*	*5–10°S*
Brazzaville[b]	*4°S*	*14°E*	*7*	*1990–1992*	*0–5°S*
Malindi[c]	*3°S*	*40°E*	*8*	*1999–2006*	*0–5°S*
Nairobi[c]	*1°S*	*37°E*	*46*	*1998–2012*	*0–5°S*
San Cristobal[c]	*1°S*	*89.6°W*	*31*	*1998–2012*	*0–5°S*
Kuala Lumpur[c]	*3°N*	*102°E*	*23*	*1998–2012*	*0–5°N*
Paramaribo[c]	*6°N*	*55°W*	*33*	*1999–2012*	*5–10°N*
Cotonou[c]	*6°N*	*2°E*	*7*	*2005–2007*	*5–10°N*
Panama[b]	*9°N*	*80°W*	*4*	*1966–1969*	*5–10°N*
Heredia[c]	*10°N*	*84°W*	*6*	*2005–2012*	*10–15°N*
Poona[b]	19°N	74°E	11	1966–1986	15–20°N
Hilo (Thompson)[c]	19°N	155°W	50	1998–2012	15–20°N
Hilo (Logan)[b]	20°N	155°W	30	1985–1993	20–25°N
Ha Noi[c]	21°N	106°E	9	2004–2012	20–25°N
Naha[b]	26°N	128°E	15	1989–1995	25–30°N
Kagoshima[b]	32°N	131°E	19	1980–1995	30–35°N
Tateno[b]	36°N	140°E	37	1980–1995	35–40°N
Azores[b]	38°N	29°W	22	1983–1995	35–40°N
Cagliari[b]	39°N	9°E	25	1968–1980	35–40°N
Boulder[b]	*40°N*	*105°W*	*27*	*1985–1993*	*40–45°N*
Sapporo[b]	*43°N*	*141°E*	*21*	*1980–1995*	*40–45°N*
Sofia[b]	*43°N*	*23°E*	*16*	*1982–1991*	*40–45°N*
Biscarosse[b]	*44°N*	*1°W*	*28*	*1976–1983*	*40–45°N*
Payerne[b]	47°N	7°E	95	1980–1993	45–50°N
Hohenpeissenberg[b]	48°N	11°E	135	1980–1993	45–50°N
Lindenberg[b]	52°N	99°E	18	1980–1995	50–55°N
Edmonton[b]	53°N	114°W	41	1980–1993	50–55°N
Goose_Bay[b]	53°N	60°W	45	1980–1993	50–55°N
Churchill[b]	59°N	147°W	43	1980–1993	55–60°N
Sodankyla[b]	67°N	27°E	20	1989–1992	65–70°N
Resolute[b]	75°N	95°W	45	1980–1993	75–80°N
Ny_Alesund[b]	79°N	12°E	19	1990–1993	75–80°N
Alert[b]	83°N	62°W	29	1988–1993	80–85°N

[a]The latitude, longitude, average number of soundings per month, and length of data record for each ozonesonde station used in the climatology is given, along with the zonal mean latitude bins (which are the same as those used for the satellite climatologies). Entries in italics show the stations that are averaged to calculate the seasonal cycle in the tropics (15°S–15°N) and northern and southern midlatitudes (40–45°N and 40–45°S) in Figure 6. We include Asp. Laverton, located at 38°S, in the calculation of the southern midlatitude seasonal cycle to avoid the use of a single station.
[b]The data are from *Logan* [1999].
[c]The data are from *Thompson et al.* [2003].

studies. In the Southern Hemisphere extratropics, the TES climatology shows positive biases of 20–30% with respect to the ozonesonde climatology for $p > 100$ hPa and negative biases of 20–30% for $p < 100$ hPa. The inconsistency between this comparison and the validation results discussed in section 2.1 likely arises from the sparse ozonesonde coverage in the Southern Hemisphere, the fact that we have not applied the TES

operator to the ozonesonde measurements, and the comparison here being limited to a single month (results for the seasonal cycle are discussed in section 3.5). For latitudes $>$ ~40°N/S and $p \leq 200$ hPa, it appears that the differences between the climatologies from the limb instruments and the TES climatology likely reflect biases in TES rather than any significant bias in the limb sounders' climatologies. The direct comparison of the satellite climatologies to TES, using the TES operational operator, results in agreement of all of the satellite climatologies at the 10% level for this region (Figure 5, fourth column). However, in reducing the difference between the limb sounders and TES, the use of the observational operator also introduces some of the TES bias into the virtual retrievals.

In the tropics, where ozone abundances are low, small absolute differences translate into large relative differences, as also seen in Figure 4. The limb-viewing instruments differ from one another and from TES by up to 90% in the tropics and subtropics (Figure 5, third column). The TES climatology does not differ systematically from the ozonesonde climatology in the tropics for $p < 200$ hPa, except at 150 hPa, where it is positively biased by ~25%. Thus, the greater ozone abundances in the limb sounder climatologies represent an overestimate of tropical ozone throughout most of the UTLS for this month. However, although differences between the annual mean climatologies are generally similar to or smaller than the differences shown here for April, the annual mean TES climatology at 150 hPa is actually biased low by $>$20% relative to the annual mean ozonesonde climatology over much of the tropics (see also section 3.5). Thus, annual mean positive differences between the limb sounder climatologies and TES seen in Figure 4 likely reflect true positive biases for the limb climatologies only for $p < 150$ hPa. With the exception of HIRDLS, which has high ozone values over a deep vertical extent (thus limiting the impact of smoothing), the TES observational operator greatly reduces the differences between the climatologies, with agreement to within ~30% in the tropics and subtropics. The comparison to TES is most robust for $p < 100$ hPa, where the virtual retrievals are relatively free of influence from the fill profile. While the annual mean pattern of differences between HIRDLS and TES is more or less centered at the equator (Figure 4), the HIRDLS climatology shows the largest differences from TES and from the other climatologies in the southern subtropics in April, suggesting perhaps a seasonal variability in the aerosol effect on the ozone retrievals.

3.5. Seasonal Cycle

Figure 6 shows the seasonal cycle of ozone in the southern midlatitudes, tropics, and northern midlatitudes averaged over 2005–2010 for the original climatologies as well as for the virtual retrievals using the TES observational operator. Dashed lines in the right column of plots for each latitude region again indicate where differences in the VTR due to the choice of fill profile exceed 50% of the difference between the VTR and TES for an instrument. The ozonesonde climatology is included in the left column for each region. The seasonal variability of ozone is largely driven by seasonal changes in the Brewer-Dobson circulation [*Folkins et al.*, 2006; *Randel et al.*, 2007]. In the midlatitudes, there is an annual cycle in ozone at all pressure levels, with maxima and minima in September and March, respectively, in the Southern Hemisphere and March and August, respectively, in the Northern Hemisphere [*Logan*, 1999]. In the tropics, there is a weak semiannual cycle driven primarily by mixing below ~150 hPa [*Konopka et al.,* 2010; *Ploeger et al.*, 2012], with maxima in June and September, transitioning to a strong single peak with a maximum in August at 100 hPa and above.

There are large differences among the climatologies in the timing and magnitude of the seasonal cycle in the tropical upper troposphere ($p \geq 100$ hPa). The OSIRIS climatology has the largest difference in peak-to-peak amplitude ($>$100%) relative to TES, while the SCIAMACHY climatology has the largest difference in timing, with a single broad peak from March to September. However, while the TES climatology seasonal cycle shows reasonable agreement with the sonde climatology at these levels (though with a general negative bias), the station-to-station variability in ozone from the sonde measurements is so large that the sonde climatology encompasses all of the satellite climatologies. The differences between the satellite climatologies are reduced in the comparison with the TES observational operator so that the differences in seasonal cycle amplitude among all of the virtual retrievals are less than 50% but are still much larger than in any other region. We note that the choice of fill profile significantly impacts most of the virtual retrievals in the tropical upper troposphere so that, combined with the large variability in the sonde climatology, our conclusions are less robust here than anywhere else. We also note that as discussed in section 3.4, the difference between the TES and ozonesonde climatologies is smaller in April than any other time of the year at 150 hPa and that the TES climatology is negatively biased with respect to the sondes for $p \geq 150$ hPa.

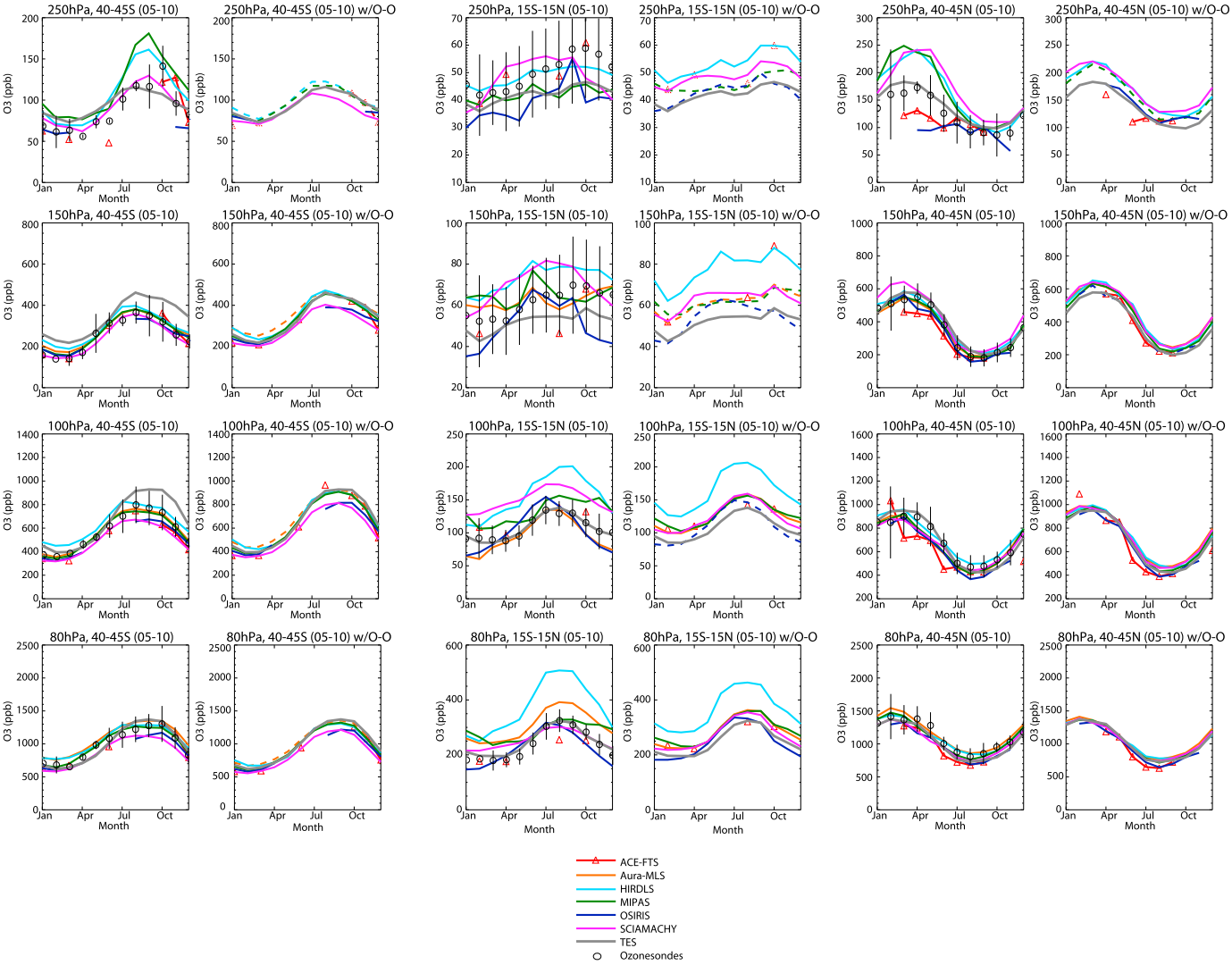

Figure 6. Seasonal cycle of ozone in the UTLS for 2005–2010. Seasonal cycle of ozone from (two left columns) 40 to 45°S, (two middle columns) 15S to 15°N, and (two right columns) 40 to 45°N at (first row) 250 hPa, (second row) 150 hPa, (third row) 100 hPa, and (fourth row) 80 hPa. The left column in each grouping shows the seasonal cycle for each climatology; the right column in each grouping shows the seasonal cycle after application of the TES observational operator. The TES measurements are the same in both left and right columns of each group. Dashed lines in the figures in the right column of each group indicate portions of the virtual retrieval where the difference in the virtual retrieval using the two different fill profiles exceeds 50% of the difference between the virtual retrieval and TES. Black circles in the left columns of each grouping show the ozonesonde climatology; vertical bars represent the standard deviation of the climatological ozonesonde measurements from the stations in each latitude band.

In the tropical lower stratosphere (70 hPa $< p \leq$ 100 hPa), there are also large discrepancies between the satellite climatologies, with differences in the magnitude of the seasonal cycle of up to 85% relative to TES for the original climatologies. Here, however, the TES seasonal cycle agrees very well with that from the ozonesondes, and the variability in the ozonesonde climatology is largely diminished. The smoothing by the TES observational operator greatly improves the consistency in the seasonal cycle amplitude (to within 20% except for HIRDLS, which differs in peak-to-peak amplitude from TES by 25–45% at these pressure levels), with the largest impact at 100 hPa. In the original data sets there are differences of up to 2 months in the timing of the ozone minimum and maximum; with the observational operator the consistency is improved to ±1 month. The changes in timing result from some combination of smoothing the seasonal cycle signal over a deep layer, with differences in phase throughout the layer, and the influence of the seasonal cycles in the TES a priori and averaging kernel.

There is excellent agreement among the satellite climatologies regarding the timing and magnitude of the seasonal cycle in northern midlatitudes for $p <$ 200 hPa; additionally, they all agree well with the ozonesonde

climatology. For all instruments except ACE-FTS (which has limited sampling), the seasonal cycle peak-to-peak amplitude is consistent to within 25% for the original climatologies and for all instruments including ACE-FTS it is consistent within <5% using the TES observational operator. At $p \geq 200$ hPa, the MIPAS, SCIAMACHY, and HIRDLS climatologies have a 50–75% larger seasonal cycle than TES, whose climatology agrees well with the sondes. However, the magnitudes of the seasonal cycle in the satellite climatologies are consistent to within 5% when they are compared with the TES observational operator, with only the MIPAS virtual retrievals being strongly dependent on the fill profile. In the southern midlatitudes, the amplitude and timing of the TES seasonal cycle agree well with the ozonesonde climatology (though with a positive bias throughout the year at 150 hPa) at all levels except 100 hPa, where the ozone maximum in the TES climatology is almost 150 ppb larger than that seen in the ozonesondes and HIRDLS, MIPAS, and Aura-MLS climatologies. At $p \leq 100$ hPa, the SCIAMACHY and OSIRIS have a 15% smaller seasonal cycle than those of the other instruments and sondes; the flatness results from an underestimate of the ozone maximum relative to the other climatologies and may be due to their limited sampling during winter. When the TES observational operator is applied to the climatologies, they agree to within 5% except for SCIAMACHY and OSIRIS. The vertical smoothing of the TES operator, in fact, spreads the low winter values in these climatologies to all of the pressure levels. We note that the increases in ozone at 150 and 100 hPa in the HIRDLS, MIPAS, and Aura-MLS virtual retrievals relative to the original climatologies represent another example of the TES operator introducing possible biases in the virtual retrievals.

3.6. Interannual Variability

Figure 7 shows the deviations from the 2005–2010 climatological monthly mean ozone for each instrument in the southern midlatitudes, tropics, and northern midlatitudes using the original climatologies as well as the virtual retrievals with the TES observational operator. As for the seasonal cycle, the differences between the climatologies are largest in the tropics, and the TES observational operator damps out much of the smaller-scale variability particularly for $p \geq 100$ hPa and greatly improves the consistency in this region. The HIRDLS climatology shows the largest differences in tropical interannual variability relative to the other instruments for $p \leq 100$ hPa, and the TES observational operator spreads the information downward so that it increases the apparent differences between HIRDLS and the other instruments for $p > 100$ hPa in the virtual retrievals. ACE-FTS also shows large differences in interannual variability from the other instruments at $p \leq 100$ hPa, likely due to its sparse sampling of the tropics. The interannual variability in OSIRIS ozone is somewhat noisier than that of the other instruments, even with the TES observational operator, but it is generally consistent with the other climatologies for $p < 100$ hPa, where the fill profile has little influence on the virtual retrieval. Overall, the interannual variability in ozone is relatively low in the tropics, as expected, and the only signal that is observed by all of the instruments is a pronounced minimum in early 2010 throughout the UTLS region. This minimum can be seen in the original climatologies and is not an artifact of the TES observational operator. The low ozone values result from changes in convection and an increase in the Brewer-Dobson circulation associated with the 2009–2010 El Niño and coincident strong easterly shear phase of the stratospheric quasi-biennial oscillation (QBO) [*Neu et al.*, 2014].

The interannual variability is more consistent between the various climatologies in the northern and southern midlatitudes than in the tropics, both in the original data sets and in the vertically smoothed virtual retrievals. As was the case for the seasonal cycle, the HIRDLS climatology and virtual retrievals agree very well with those from the other instruments in midlatitudes, despite their large differences from the other instruments in the tropics. The largest discrepancies in midlatitude interannual variability can be seen in the climatologies from ACE-FTS and OSIRIS in the Southern Hemisphere. In the case of ACE-FTS, the sampling is likely to blame, though we note that there may be a contribution from the fact that the lowest retrieval level (and thus the influence of the fill profile) varies throughout the year and between years more for ACE-FTS than for any other instrument. OSIRIS does not continuously sample the 40°–45°S latitude band so that the climatological monthly mean and deviations from the mean are not well defined in Southern Hemisphere winter. The TES observational operator reduces the ozone variability somewhat in midlatitudes, but the major deviations in northern midlatitude ozone in 2008 and 2010 are well preserved, except during the January–April 2010 TES data gap. The northern midlatitude ozone minimum in 2008 and maximum in 2010 result from changes in the Brewer-Dobson circulation associated with La Niña/westerly shear QBO and El Niño/easterly shear QBO, respectively [*Neu et al.*, 2014]. In the southern midlatitudes, the climatologies all show maxima in 2005 and 2007 and minima in 2006 at $p \leq 100$ hPa. The TES observational operator reduces the maxima in the virtual retrievals due to the vertical smearing. TES stopped sampling south of 30°S in January 2010.

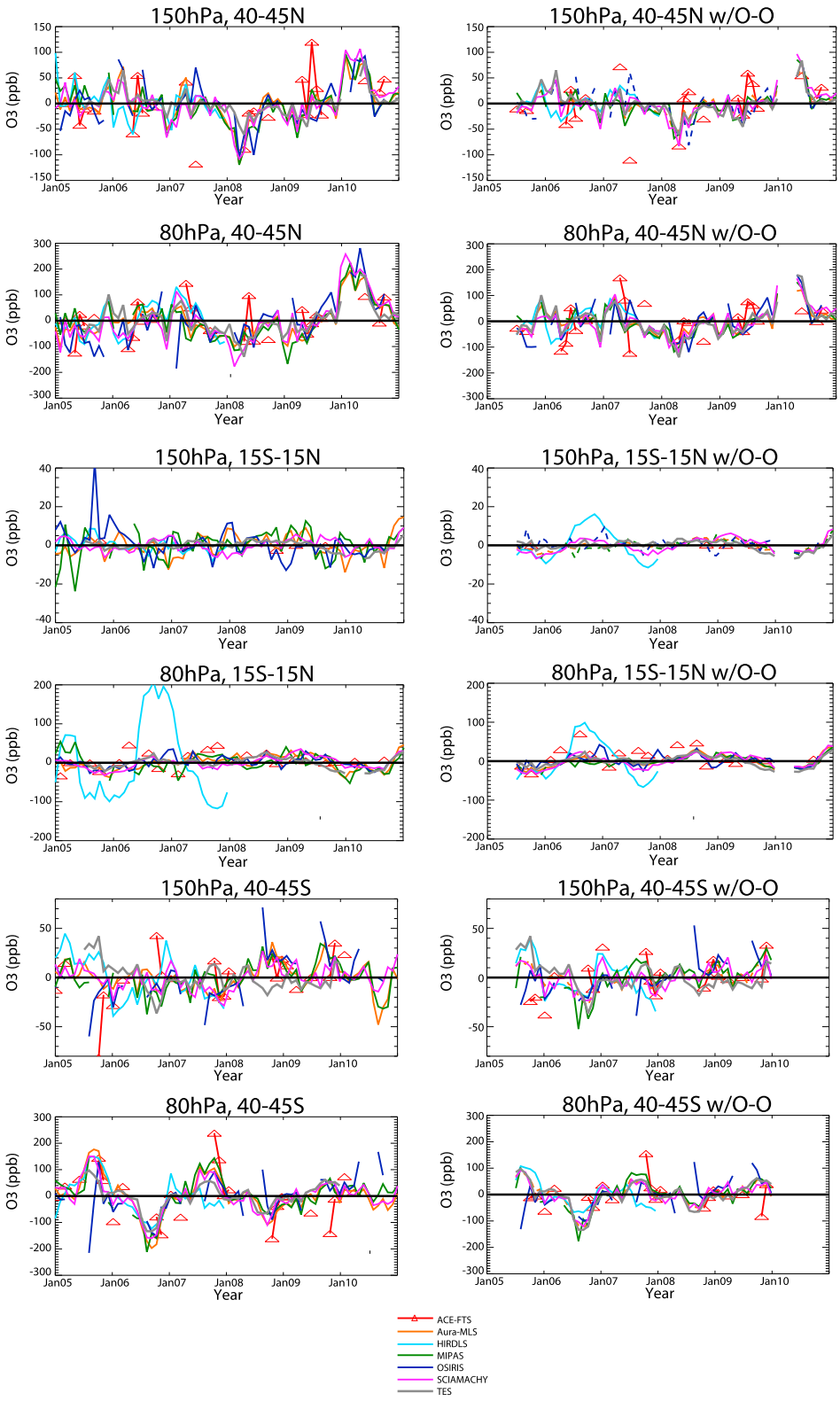

Figure 7. Interannual variability of ozone in the UTLS for 2005–2010. Deseasonalized ozone anomalies at 150 hPa and 80 hPa for (first and second rows) 40–45°N, (third and fourth rows) 15°S–15°N, and (fifth and sixth rows) 40–45°S. (left column) The original climatologies; (right column) the climatologies after application of the TES observational operator. Dashed lines in the figures in Figure 7 (right column) indicate portions of the virtual retrieval where the difference in the virtual retrieval using the two different fill profiles exceeds 50% of the difference between the virtual retrieval and TES.

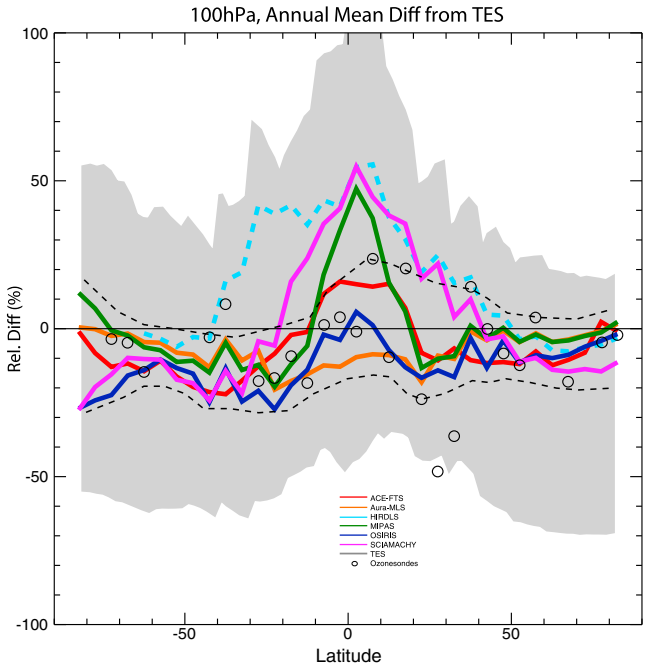

Figure 8. Meridional profile of differences between ACCMIP models/SPARC Data Initiative climatologies and TES for 2005–2010. Grey shaded region shows the range of relative differences in 100 hPa annual mean zonal mean ozone between the ACCMIP models and TES ((Model − TES)/TES) from *Bowman et al.* [2013]. The TES observational operator has not been applied to the model output because it was not used in the original study. Colored lines show the differences between the SPARC Data Initiative climatologies and TES, and black circles represent the ozonesonde climatology relative difference from TES. Black dashed lines show the range of ozone consistent with a preponderance of the observational climatologies at each latitude.

4. Discussion

While the use of zonal mean climatologies for detailed UTLS process studies is obviously limited, the SPARC Data Initiative climatologies nevertheless represent our best knowledge of the abundance and temporal variability of ozone in the UTLS, and the characterization of the data sets presented here will provide valuable information for model evaluation. For example, a recent paper examined climatological differences in ozone between the suite of Atmospheric Chemistry and Climate Model Intercomparison Project (ACCMIP) models and TES and found that large biases in the models' UTLS ozone relative to TES correspond to biases in ozone's effect on outgoing longwave radiation (OLR) exceeding 10 mW/m^2 [*Bowman et al.*, 2013]. However, the biases and uncertainties of the TES measurements were not considered in the study. Figure 8 shows the range of differences in annual mean zonal mean ozone between the models and TES as a function of latitude at 100 hPa. The TES observational operator has not been applied to the models because it was not used in the original analysis. The models differ from TES by up to a factor of 2 in either direction (differences between the stratosphere-focused Chemistry-Climate Model Validation 2 (CCMVal-2) project models and observations were similar in magnitude in the tropics and ~10% smaller in the extratropics [*SPARC CCMVal*, 2010]). The relative differences between the original satellite climatologies, as well as the ozonesonde climatology, and TES are also shown and are much smaller than the model-TES differences at all latitudes. The measurements thus provide meaningful constraints for the models. The black dashed lines represent a "best estimate range" for ozone (defined by including a preponderance of the measurements) based on the measurement climatologies and could be used to quantitatively evaluate the models with a robust characterization of the uncertainty in our knowledge of the ozone abundances. We note that the uncertainty range could be further reduced by accounting for differences in vertical resolution between the climatologies (applying the TES observational operator to both the satellite and ozonsonde climatologies) and accounting for the sparse sampling of the ozonesonde climatology. The range of model differences from TES would likewise be reduced by applying the observational operator but would still be much larger than the measurement range.

The characterization of the SPARC Data Initiative climatologies presented here can also be used to provide robust quantification of the seasonal cycle in ozone in the UTLS, which has been used to evaluate model representation of transport and photochemistry [e.g., *SPARC CCMVal*, 2010; *Gettelman et al.*, 2010; *Hegglin et al.*, 2010]. The seasonal cycle of ozone near the tropical tropopause (~100 hPa) is determined by chemical production, vertical transport, and mixing in of extratropical air, and the amplitude and phase reflect variations in the relative contributions of these processes. While the climatologies differ in amplitude by up to 85% at 100 hPa in the tropics, the peak-to-peak amplitude of the seasonal cycle in the CCMVal-2 models varied by a factor of >5 at 100 hPa in the same region, and two of the models misrepresented the phase by >4 months [*SPARC CCMVal*, 2010; *Gettelman et al.*, 2010]. In the extratropical lowermost stratosphere,

the seasonal cycle has been used to evaluate the balance between the large-scale stratospheric circulation, which carries photochemically aged air downward into the region [*Logan*, 1999], and the breaking of synoptic-scale waves above the subtropical jet that brings in "young" tropical air masses [e.g., *SPARC CCMVal*, 2010; *Hegglin et al.*, 2010]. These processes together act to determine the distribution of radiatively active species in the UTLS.

The CCMVal-2 models reproduce the 100 hPa seasonal cycle in midlatitudes much more consistently than in the tropics but still vary in peak-to-peak amplitude by almost a factor of 2, while the measurements agree to within 15% (with the exception of TES in the southern midlatitudes). This analysis provides a well-characterized data set for quantitative evaluation of model representation of the ozone seasonal cycle, as well as El Niño–Southern Oscillation/QBO variability in midlatitude ozone (section 3.6), for future studies.

5. Summary and Conclusions

We have presented the first comprehensive intercomparison of the currently available satellite climatologies in the UTLS region. Comparing climatologies from instruments with different viewing geometries, sampling patterns, and vertical resolution requires methodologies that account for these differences, particularly in regions with strong trace gas gradients such as the UTLS. To compare the monthly mean, zonal mean ozone climatologies from the SPARC Data Initiative, we used the TES observational operator to vertically smooth the climatologies from the higher-resolution limb-viewing instruments. This approach provides a common basis for comparison of the large-scale ozone morphology as well as the seasonal and interannual variability of ozone within the UTLS. However, our approach has several limitations, including the fact that the virtual retrievals can be sensitive to how one chooses to "fill in" the profiles below lowest measurement level of the limb sounders, that the TES sensitivity varies in the UTLS such that the a priori profile has a significant influence near 150 hPa in the extratropics, and that the averaging kernels are not fully independent of the ozone abundance, resulting in errors in the virtual retrievals that are difficult to quantify. We have tried to account for these factors when possible and to focus on robust differences in the UTLS climatologies.

The TES observational operator smoothes small-scale ozone structures and due to the influence of the a priori tends to increase tropical-extratropical ozone gradients as well as midlatitude vertical ozone gradients in the climatologies from the limb-viewing instruments. It also reduces and vertically smoothes the differences between the limb climatologies and TES. The TES observational operator reduces the temporal variability of the ozone climatologies from the high-resolution instruments but also greatly improves the consistency between them. This indicates that the differences in vertical resolution among the limb-viewing instruments make a substantial contribution to differences in their retrieved ozone distributions both relative to TES and relative to one other.

Most of the limb-viewing instruments have climatological mean positive differences (ranging from 5 to 75%) relative to TES ozone in the tropics, though for several instruments the differences depend strongly on the fill profile below ~100 hPa. For $p \leq 100$ hPa, the positive difference from TES likely reflect true positive biases for the climatologies given TES's lack of bias with respect to the ozonsonde climatology. In the Northern Hemisphere extratropics, only the HIRDLS and MIPAS climatologies have differences with respect to TES that are $>$15% and are also independent of the fill profile (Figure 4). In the southern extratropics, the TES observational operator greatly reduces differences between the limb sounder climatologies and TES due to TES's low sensitivity at the pressure levels where the differences between the original climatologies and TES are largest.

There are large differences in the timing and magnitude of the seasonal cycle in the tropical upper troposphere, though the amplitude differences are only ~1/3 those seen in models. At $p \leq 100$ hPa, the climatologies show a more consistent tropical seasonal cycle, particularly when smoothed to the TES vertical resolution. The TES observational operator reduces the differences in seasonal cycle amplitude to within 20% of TES for all instruments except HIRDLS. In general, there is very good agreement among the climatologies regarding both the timing and magnitude of the seasonal cycle in midlatitudes, except that ozone from the OSIRIS and SCIAMACHY climatologies is ~15% low relative to the other instruments during the southern midlatitude maximum, likely due to their limited sampling of this region. All of the climatologies show low interannual variability in the tropics (except for HIRDLS) and higher variability in midlatitudes, with northern midlatitude interannual variability greatly exceeding that in southern midlatitudes for $p > 80$ hPa. The sampling of the

ACE-FTS instrument is insufficient to capture interannual variability on monthly time scales in the tropics. The TES observational operator greatly reduces the interannual variability in ozone from the limb sounder climatologies for $p > 100$ hPa in the tropics and $p > 200$ hPa in midlatitudes. This improves the consistency between the data sets but may limit the usefulness of the virtual retrievals for quantifying UTLS variability.

This work represents an important first step in assessing the differences between satellite climatologies in the UTLS region and provides a template for comparison of measurements from limb- and nadir-viewing instruments. It also provides a well-characterized data set for model evaluation of zonal mean ozone abundances and the seasonal and interannual variability of ozone. However, a much more detailed UTLS intercomparison using high spatial and temporal resolution measurements of multiple species is needed to fully characterize differences between instruments in this region and has been proposed as a follow on to the SPARC Data Initiative. It will require diagnostic tools that minimize geophysical variability and differences in sampling and resolution such as tracer-tracer correlations, probability distribution functions, tropopause-relative vertical coordinates, and jet-based coordinates [e.g., *Hegglin et al.*, 2008; *SPARC CCMVal*, 2010; *Manney et al.*, 2011]. Such an analysis promises to not only provide a detailed assessment of the quality of the satellite data but also to improve our understanding of UTLS structure and processes.

Acknowledgments

The authors thank the relevant instrument teams and space agencies for their data and support. We also thank the ISSI in Bern for facilitating two successful team meetings in Bern as part of the ISSI International Team activity program, and the SPARC Toronto office and SPARC/WCRP for travel support. Work at the Jet Propulsion Laboratory, California Institute of Technology, was performed under contract from the National Aeronautics and Space Administration. John Gille and the work of the HIRDLS team in the U.S. was supported by NASA contract NAS5-97046. Michaela I Hegglin's work within the SPARC Data Initiative was supported by the CSA and ESA. IAA was supported by the Spanish MINECO under grant AYA2011-23552 and EC FEDER funds. The work of the University of Bremen team on the SCIAMACHY ozone climatology was funded in part by the German Aerospace Agency (DLR) within the project SADOS (50EE1105) and by the state and University of Bremen. ACE is a Canadian-led mission mainly supported by the Canadian Space Agency (CSA). Development of the ACE-FTS climatologies was supported by grants from the Canadian Foundation for Climate and Atmospheric Sciences and the CSA. The ozonesonde climatology and ACCMIP model results were provided by Paul Young of Lancaster University and Kevin Bowman of the Jet Propulsion Laboratory, respectively.

References

Aghedo, A. M., K. W. Bowman, D. T. Shindell, and G. Faluvegi (2011), The impact of orbital sampling, monthly averaging and vertical resolution on climate chemistry model evaluation with satellite observations, *Atmos. Chem. Phys.*, *11*(13), 6493–6514, doi:10.5194/acp-11-6493-2011.

Beer, R. (2006), TES on the aura mission: Scientific objectives, measurements, and analysis overview, *IEEE Trans. Geosci. Remote Sens.*, *44*(5), 1102–1105, doi:10.1109/TGRS.2005.863716.

Beer, R., T. A. Glavich, and D. M. Rider (2001), Tropospheric emission spectrometer for the Earth Observing System's Aura satellite, *Appl. Opt.*, *40*, 2356–2367, doi:10.1364/AO.40.002356.

Bowman, K. W., T. Steck, H. M. Worden, J. Worden, S. Clough, and C. Rodgers (2002), Capturing time and vertical variability of tropospheric ozone: A study using TES nadir retrievals, *J. Geophys. Res.*, *107*(D23), 4723, doi:10.1029/2002JD002150.

Bowman, K. W., et al. (2006), Tropospheric Emission Spectrometer: Retrieval method and error analysis, *IEEE Trans. Geosci. Remote Sens.*, *44*(5), 1297–1307, doi:10.1109/TGRS.2006.871234.

Bowman, K. W., et al. (2013), Evaluation of ACCMIP outgoing longwave radiation from tropospheric ozone using TES satellite observations, *Atmos. Chem. Phys.*, *13*, 4057–4072, doi:10.5194/acp-13-4057-2013.

Boxe, C. S., et al. (2010), Validation of northern latitude Tropospheric Emission Spectrometer stare ozone profiles with ARC-IONS sondes during ARCTAS: Sensitivity, bias and error analysis, *Atmos. Chem. Phys.*, *10*, 9901–9914, doi:10.5194/acp-10-9901-2010.

Degenstein, D. A., A. E. Bourassa, C. Z. Roth, and E. J. Llewellyn (2009), Limb scatter ozone retrieval from 10 to 60 km using a multiplicative algebraic reconstruction technique, *Atmos. Chem. Phys.*, *9*(17), 6521–6529, doi:10.5194/acp-9-6521-2009.

Dupuy, E., et al. (2009), Validation of ozone measurements from the Atmospheric Chemistry Experiment (ACE), *Atmos. Chem. Phys.*, *9*(2), 287–343, doi:10.5194/acp-9-287-2009.

Folkins, I., P. Bernath, C. Boone, G. Lesins, N. Livesey, A. M. Thompson, K. Walker, and J. C. Witte (2006), Seasonal cycles of O_3, CO, and convective outflow at the tropical tropopause, *Geophys. Res. Lett.*, *33*, L16802, doi:10.1029/2006GL026602.

Forster, P. M., and K. P. Shine (2002), Assessing the climate impacts of trends in stratospheric water vapour, *Geophys. Res. Lett.*, *29*, 1086–1089, doi:10.1029/2001GL013909.

Froidevaux, L., et al. (2008), Validation of Aura Microwave Limb Sounder stratospheric ozone measurements, *J. Geophys. Res.*, *113*, D15S20, doi:10.1029/2007JD008771.

Funke, B., and T. von Clarmann (2012), How to average logarithmic retrievals?, *Atmos. Meas. Tech.*, *5*(4), 831–841, doi:10.5194/amt-5-831-2012.

Gettelman, A., et al. (2010), Multimodel assessment of the upper troposphere and lower stratosphere: Tropics and global trends, *J. Geophys. Res.*, *115*, D00M08, doi:10.1029/2009JD013638.

Gettelman, A., P. Hoor, L. L. Pan, W. J. Randel, M. I. Hegglin, and T. Birner (2011), The extra tropical upper troposphere and lower stratosphere, *Rev. Geophys.*, *49*, RG3003, doi:10.1029/2011RG000355.

Gille, J., et al. (2008), High Resolution Dynamics Limb Sounder: Experiment overview, recovery, and validation of initial temperature data, *J. Geophys. Res.*, *113*, D16S43, doi:10.1029/2007JD008824.

Hegglin, M. I., C. D. Boone, G. L. Manney, T. G. Shepherd, K. A. Walker, P. F. Bernath, W. H. Daffer, P. Hoor, and C. Schiller (2008), Validation of ACE-FTS satellite data in the upper troposphere/lower stratosphere (UTLS) using non-coincident measurements, *Atmos. Chem. Phys.*, *8*, 1483–1499, doi:10.5194/acp-8-1483-2008.

Hegglin, M. I., C. D. Boone, G. L. Manney, and K. A. Walker (2009), A global view of the extratropical tropopause transition layer from Atmospheric Chemistry Experiment Fourier transform spectrometer O_3, H_2O, and CO, *J. Geophys. Res.*, *114*, D00B11, doi:10.1029/2008JD009984.

Hegglin, M. I., et al. (2010), Multi-model assessment of the upper troposphere and lower stratosphere: Extra-tropics, *J. Geophys. Res.*, *115*, D00M09, doi:10.1029/2010JD013884.

Jiang, Y. B., et al. (2007), Validation of Aura Microwave Limb Sounder ozone by ozonesonde and lidar measurements, *J. Geophys. Res.*, *112*, D24S34, doi:10.1029/2007JD008776.

Jones, D. B. A., K. W. Bowman, J. A. Logan, C. L. Heald, J. Liu, M. Luo, J. Worden, and J. Drummond (2009), The zonal structure of tropical O_3 and CO as observed by the Tropospheric Emission Spectrometer in November 2004. Part I. Inverse modeling of CO emissions, *Atmos. Chem. Phys.*, *9*, 3547–3562, doi:10.5194/acp-9-3547-2009.

Konopka, P., J. U. Grooß, G. Günther, F. Ploeger, R. Pommrich, R. Müller, and N. Livesey (2010), Annual cycle of ozone at and above the tropical tropopause: Observations versus simulations with the Chemical Lagrangian Model of the Stratosphere (CLaMS), *Atmos. Chem. Phys.*, *10*, 121–132, doi:10.5194/acp-10-121-2010.

Kulawik, S. S., et al. (2006), TES atmospheric profile retrieval characterization: An orbit of simulated observations, *IEEE Trans. Geosci. Remote Sens.*, *44*(5), 1324–1332, doi:10.1109/TGRS.2006.871207.

Logan, J. A. (1999), An analysis of ozonesonde data for the troposphere: Recommendations for testing 3-D models, and development of a gridded climatology for tropospheric ozone, *J. Geophys. Res.*, *104*, 16,115–16,149, doi:10.1029/1998JD100096.

Manney, G. L., et al. (2011), Jet characterization in the upper troposphere/lower stratosphere (UTLS): Applications to climatology and transport studies, *Atmos. Chem. Phys.*, *11*, 6115–6137, doi:10.5194/acp-11-6115-2011.

Mieruch, S., et al. (2012), Global and long-term comparison of SCIAMACHY limb ozone profiles with correlative satellite data (2002–2008), *Atmos. Meas. Tech.*, *5*(4), 771–788, doi:10.5194/amt-5-771-2012.

Nardi, B., et al. (2008), Initial validation of ozone measurements from the High Resolution Dynamics Limb Sounder, *J. Geophys. Res.*, *113*, D16S36, doi:10.1029/2007JD008837.

Nassar, R., et al. (2008), Validation of Tropospheric Emission Spectrometer (TES) nadir ozone profiles using ozonesonde measurements, *J. Geophys. Res.*, *113*, D15S17, doi:10.1029/2007JD008819.

Neu, J. L., T. Flury, G. L. Manney, M. L. Santee, N. J. Livesey, and J. Worden (2014), Tropospheric ozone variations governed by changes in stratospheric circulation, *Nature Geosci.*, *7*, 340–344, doi:10.1038/ngeo2138.

Peevey, T. R., J. C. Gille, C. E. Randall, and A. Kunz (2012), Investigation of double tropopause spatial and temporal global variability utilizing High Resolution Dynamics Limb Sounder temperature observations, *J. Geophys. Res.*, *117*(D01), 105, doi:10.1029/2011JD016443.

Ploeger, F., P. Konopka, R. Müller, S. Fueglistaler, T. Schmidt, J. C. Manners, J.-U. Grooß, G. Günther, P. M. Forster, and M. Riese (2012), Horizontal transport affecting trace gas seasonality in the Tropical Tropopause Layer (TTL), *J. Geophys. Res.*, *117*, D09303, doi:10.1029/2011JD017267.

Randel, W. J., M. Park, F. Wu, and N. Livesey (2007), A large annual cycle in ozone above the tropical tropopause linked to the Brewer-Dobson circulation, *J. Atmos. Sci.*, *64*, 4479–4488, doi:10.1175/2007JAS2409.1.

Rodgers, C. (2000), *Inverse Methods for Atmospheric Sounding: Theory and Practice*, World Scientific, London.

Rodgers, C. D., and B. J. Connor (2003), Intercomparison of remote sounding instruments, *J. Geophys. Res.*, *108*(D3), 4116, doi:10.1029/2002JD002299.

Solomon, S., et al. (Eds.) (2007), *Contribution of Working Group I to the Fourth Assessment Report of the Intergovernmental Panel on Climate Change, 2007*, Cambridge Univ. Press, Cambridge.

Stratosphere-troposphere Processes and their Role in Climate Chemistry-Climate Model Validation (SPARC CCMVal) (2010), SPARC CCMVal report on the evaluation of Chemistry-Climate Models, *SPARC Rep. 5, WCRP-132, WMO/TD-1526*, edited by D. W. Waugh, V. Eyring, and T. G. Shepherd, Zurich, Switzerland.

Tegtmeier, S., et al. (2013), SPARC Data Initiative: A comparison of ozone climatologies from international satellite limb sounders, *J. Geophys. Res. Atmos.*, *118*, 12,229–12,247, doi:10.1002/2013JD019877.

Thompson, A. M., et al. (2003), Southern Hemisphere Additional Ozonesondes (SHADOZ) 1998–2000 tropical ozone climatology 1. Comparison with Total Ozone Mapping Spectrometer (TOMS) and ground-based measurements, *J. Geophys. Res.*, *108*(D2), 8238, doi:10.1029/2001JD000967.

Toohey, M., et al. (2013), Characterizing sampling biases in the trace gas climatologies of the SPARC Data Initiative, *J. Geophys. Res. Atmos.*, *118*, 11,847–11,862, doi:10.1002/jgrd.50874.

Verstraeten, W. W., K. F. Boersma, J. Zörner, M. A. F. Allaart, K. W. Bowman, and J. R. Worden (2013), Validation of six years of TES tropospheric ozone retrievals with ozonesonde measurements: Implications for spatial patterns and temporal stability in the bias, *Atmos. Meas. Tech.*, *6*, 1413–1423, doi:10.5194/amt-6-1413-2013.

von Clarmann, T., et al. (2009), Retrieval of temperature, H2O, O3, HNO3, CH4, N2O, ClONO2 and ClO from MIPAS reduced resolution nominal mode limb emission measurements, *Atmos. Meas. Tech.*, *2*(1), 159–175, doi:10.5194/amt-2-159-2009.

Worden, H. M., et al. (2007), Comparisons of Tropospheric Emission Spectrometer (TES) ozone profiles to ozonesondes: Methods and initial results, *J. Geophys. Res.*, *112*, D03309, doi:10.1029/2006JD007258.

Worden, H. M., K. W. Bowman, J. R. Worden, A. Eldering, and R. Beer (2008), Satellite measurements of the clear-sky greenhouse effect from tropospheric ozone, *Nat. Geosci.*, *1*, 305–308, doi:10.1038/ngeo182.

Worden, H. M., K. W. Bowman, S. S. Kulawik, and A. M. Aghedo (2011), Sensitivity of outgoing longwave radiative flux to the global vertical distribution of ozone characterized by instantaneous radiative kernels from Aura TES, *J. Geophys. Res.*, *116*, D14115, doi:10.1029/2010JD015101.

Worden, J. S., S. S. Kulawik, M. Shepard, S. Clough, H. Worden, K. Bowman, and A. Goldman (2004), Predicted errors of Tropospheric Emission Spectrometer nadir retrievals from spectral window selection, *J. Geophys. Res.*, *109*, D09308, doi:10.1029/2004JD004522.

World Meteorological Organization (2011), Scientific Assessment of Ozone Depletion: 2010, Global Ozone Research and Monitoring Project-Report 52, 516 pp., Geneva, Switzerland.